J Mater Sci (2007) 42:6018–6026
DOI 10.1007/s10853-006-0970-2

Beach sand from Cancun Mexico: a natural macro- and mesoporous material

Hui Chen · Jinhai Wang · Zia ur Rahman · James G. Worden · Xiong Liu · Qiu Dai · Qun Huo

Received: 27 February 2006 / Accepted: 13 September 2006 / Published online: 6 April 2007

Abstract Sand particles from Cancun, Mexico were studied using a number of advanced spectroscopic and microscopic techniques. The main chemical composition of sand particles was confirmed to be calcium carbonate by X-ray photoelectron spectroscopy and IR spectroscopic analysis. X-ray diffraction analysis revealed that the sand particles are aragonite, which has an Orthorhombic—Dipyramidal crystal structure. The morphological study of the sand particles by scanning electron microscopy and transmission electron microscopy revealed the presence of a highly porous channel-like structure in the sand particles. The sorption isotherm indicates that Cancun sand is a mesoporous material. The specific surface area of Cancun sand was determined to be 2.259 m^2/g by BET measurement, which is significantly higher than that of Florida sand and other forms of natural aragonite and calcite. Furthermore, it was found that the porous sand particles can adsorb gold nanoparticles of the size of a few nanometers very efficiently. The distribution of gold nanoparticles demonstrated a channel-like porous inner structure of the sand particles. We also prepared a polymer composite material by mixing the sand particles with a poly(methyl methacrylate) matrix. SEM analysis of the composite materials showed a good interfacial adhesion between sand particles and polymer matrix. These results suggest that Cancun sand, as a natural macro- and mesoporous material, may find promising applications in filtration, pollution control, composite materials and biomaterials development.

Electronic supplementary material The online version of this article (doi:10.1007/s10853-006-0970-2) contains supplementary material, which is available to authorized users.

H. Chen · J. Wang · J. G. Worden · X. Liu · Q. Dai · Q. Huo (✉)
Nanoscience Technology Center, Department of Chemistry, Department of Mechanical Materials, and Aerospace Engineering, University of Central Florida, 12424 Research Parkway, Suite 400, Orlando, FL 32826, USA
e-mail: qhuo@mail.ucf.edu

Z. ur Rahman
Materials Characterization Facility, Advanced Materials Processing & Analysis Center (AMPAC), University of Central Florida, 12443 Research Pkwy Suite 304, Orlando, FL 32826, USA

Introduction

Porous materials are very important for catalysis, separation, hydrogen storage, water purification, biomedical and many other applications [1–7]. Recently, a great amount of effort has been invested on the synthesis of porous materials [1, 8–14]. Successes have been achieved in preparing not only porous metal oxides, but also porous membranes [8], porous semiconductors [9] and even metal-organic porous crystals [1, 10–14]. However, the cost of synthetic porous materials is generally high and the disposal of these synthetic materials after use may cause significant burden to the environment.

On the other hand, nature has produced many porous materials. For example, diatomaceous earth, natural porous silica which is primarily composed of the fossilized remains of Diatoms, has been extensively used as filtering agent, absorbent and insulating material in industry [15–18]. Another highly porous materials coming from nature, charcoal, is used routinely for water treatment, purification and air filtering [19, 20]. Corals and some sea shells are currently being studied extensively as potential biomaterials for artificial bone development [21, 22]. Natural porous materials are environmentally friendly,

abundant, low cost, and in many cases recyclable. The search for and study of new natural porous materials will continue to be an interesting and important venue in materials research.

Beach sand from Cancun, Mexico has recently caught our attention as a natural porous material. Cancun, Mexico is well known for its white sand, turquoise sea water, and soft beach. It has been noticed by many people that the sand from this area is very ''sticky'' to human skin and cannot be easily washed off after swimming. A close examination of a sand sample shows that some sand particles do not wet very well in water. As a comparison, sand samples collected from other geographical locations such as different areas along Florida coast behave quite differently. This unique property of Cancun sand stimulated a great interest from us as a material. In composite material research, it is well known that a good adhesion between filler particles and a polymer matrix plays a vital role in determining the properties of a composite material. The ''sticky'' nature of Cancun sand prompted us to believe that Cancun sand may be a good filler material for composite material development. Before any potential application can be further explored, the first step is to obtain a better knowledge on the structure and properties of Cancun sand particles. However, to our knowledge, other than the fact that the main chemical component of Cancun sand is calcium carbonate [23], there is not much information available on the structure and morphology of this natural material.

In present work, we used a number of advanced microscopic and spectroscopic techniques including X-ray photoelectron spectroscopy (XPS), X-ray diffraction, scanning electron microscope (SEM), focused ion beam (FIB), transmission electron microscopy (TEM) and Infrared spectroscopy (IR) to conduct a systematic analysis on the chemical composition, surface morphology and internal structures of Cancun sand. These studies revealed that Cancun sand is a macro- to mesoporous material. The porous nature of sand particles was further confirmed by BET measurement and a nanoparticle adsorption experiment. We also prepared a composite material by mixing ground Cancun sand particles with PMMA and found a good interfacial adhesion between the sand particles and the polymer. These results suggest that Cancun sand may find important applications in filtration, pollution control, and composite material development.

Experimental

Sand sample

Cancun sand sample was collected from the beach area near the Gran Melia resort in Cancun, Mexico. Florida sand was collected from Daytona Beach. The particles were washed with deionized water and dried in air. A porcelain mortar was used to grind sand into smaller particles for studies involving the observation of internal structures of the sand. Florida sand samples collected at Daytona Beach area were used in some comparison studies. Florida sand samples were cleaned and processed in the same way as the Cancun sand before analysis and study.

X-ray photoelectron spectroscopy (XPS)

XPS spectra were obtained in a Phi 5400 XPS system equipped with an Mg K_α source (1253.6 eV, 300 W) under a base pressure of 8×10^{-9} torr. For XPS measurement, the pass energy of the analyzer was fixed to 35.75 eV. The binding energy scale of spectrometer was calibrated by using Au $4f_{7/2}$ = 84.0 eV and Cu $2p_{3/2}$ = 932.67 eV. Peak fitting was carried out by employing a symmetric Gauss-Lorentz sum function. The spin-orbit splitting was set at 3.55 eV for Ca 2p signals with a constant respective intensity ratio of 2:1 and 1.79 eV for Sr 3d and 0.69 eV for As 3d signals with a constant respective intensity ratio of 3:2. Before peak fitting, a Shirley background was subtracted.

The percentages of elements were determined by normalized XPS areas: C1s peak for carbon, Ca 2p peak for calcium, O 1s peak for oxygen, Si 2p peak for silicon, Sr 3d peak for Strontium and As 3d peak for arsenic. The integrated peak area of the corresponding XPS peak is then divided by the sensitivity factor for the given element to obtain the normalized peak area. The sensitivity factors listed in Table 1 were taken from ref. [24].

Scanning electron microscope (SEM)

The specimens were coated with a Pd-Au film by an Emitech Magnetron Sputter Coater before imaging in order to avoid electric charge build-up. The specimens then were observed by a JEOL 6400 SEM at an accelerating voltage of 5 kV.

Transmission Electron Microscopy (TEM) and Focused Ion Beam (FIB)

The cross-section of the sand particles was investigated by a FEI Tecnai F30 TEM. It is equipped with a field emission gun (FEG) and can operate at an accelerating voltage of 300 kV. It also includes an energy dispersive X-ray detector for energy dispersive X-ray spectroscopy (EDXS) elemental analysis. The spot size is about 0.3 nm for the element analysis. The atomic percentage of elements was determined by the Cliff-Lorimer ratio technique [25], which is a standard technique for TEM/EDXS quantitive analysis. No further correction was applied.

Table 1 Peak area analysis of X-ray photoelectron spectrum of sand particles

	BE (eV)	Area	Sensitivity factor	Normalized area	Atom%
C 1s	289.3	303.18	0.296	1024.24	13.11
O 1s	531.5	3667.22	0.711	5157.83	66.00
Ca 2p	347.3	1940.71	1.634	1187.71	15.20
Si 2p	102.1	59.48	0.283	210.16	2.69
Sr 3d	132.8	43.31	1.578	27.45	0.35
As 3d	43.3	118.53	0.57	207.94	2.66
Total				7815.33	100.00

The cross-section with a thickness less than 0.5 μm for TEM image was prepared with an FEI 200 TEM Focused Ion Beam instrument with the ''lift-out'' technique refined by Giannuzzi et al. [26, 27]. First, a platinum coating was deposited to cover a narrow rectangular section of the particle surface, protecting this area from the focused ion beam milling. Two deep trenches were then milled out on either sides of the coated section from top by focused ion beam with 500 pA current. In the middle, the cross-section was cut out and transferred onto a standing slot TEM grid. The sample was further thinned into electron transparency with a ~100 pA beam current from glancing angles, which became suitable for TEM analysis (see Supporting Information).

Specific surface area and pore diameter measurement

The specific surface area and pore volume-based median pore diameter was measured by the Brunauer–Emmett–Teller (BET) method with a Quadrasorb SI Surface Area and Pore Size Analyzer (Quantachrome Instruments, measurement and analysis conducted by this company as well). In the experiment, ~1.0 g of sand sample was used. The sample was degassed at 473 K under pressure of 1×10^{-4} mbar for 16 h prior to the nitrogen adsorption at 77.3 K. The cross-sectional area of N_2 used is 0.162 nm^2. The specific surface area was obtained by analysis of multi-point BET data [28]. The pore volume and average pore size is determined by Barrett–Joyner–Halenda (BJH) method [29], which is based on a modification of classic Kelvin equation and widely used in pore size analysis of mesoporous materials.

Nanoparticle adsorption study

The butanethiol-stabilized gold nanoparticles with an average core diameter around 2–3 nm (synthesized in our lab) [30] were used to test the adsorption and diffusion of nanoparticles into the pores of sand particles. A total of 0.3 g grounded sand was mixed with 1 mL nanoparticle solution in dichloromethane (0.25 wt%). After 24 h, the sand was filtered and washed by a copious amount of dichloromethane. The sand particles were then dried in air. The thin cross-section of the sand particles with gold nanoparticles was prepared by the FIB technique and examined with TEM.

Preparation of Cancun sand–polymer composite films

A 30 wt% of poly(methyl methacrylate) (PMMA) solution was prepared by dissolving PMMA powder (Aldrich, average molecular weight of 120,000 g/mol) in acetonitrile. The sand particles were ground by a porcelain mortar and then dispersed in PMMA solution. The mixture was sonicated for at least 5 min to obtain a better dispersion. The PMMA/gold nanoparticle solution was cast by a drawdown bar (Paul N. Gardner Company, Inc) on a glass substrate at 30 mils. Films were obtained after drying at least overnight in ambient conditions. The dried film was cut by a knife and the resulted cross-section was examined by SEM.

Infrared spectroscopy

The infrared spectrum of the ground Cancun sand was recorded using a PerkinElmer Spectrum^{TM} 100 FT-IR spectrometer with universal ATR sampling Accessory. The crystal is made of diamond. The sand powder sample was placed on a diamond coated ZnSe crystal (d = 1 mm) and was pressed by a pressure arm to achieve good contact between sample and crystal during measurement. A background was taken without sample before each measurement.

X-ray diffraction (XRD)

The ground sand sample was screened by a 75 μm sieve and then analyzed by using a Rigaku X-ray diffractometer with Cu K_α radiation (λ = 0.15406 nm) at 40 kV and 30 mA settings. The XRD patterns were recorded in the 2θ range of 10°–80°. The data were then analyzed with JADE7-XRD pattern processing, identification and quantification software.

Results and discussion

Chemical composition

The chemical composition of Cancun sand sample was analyzed by FT-IR spectroscopy and XPS. While FT-IR spectrum gives the bulky chemical composition, XPS study of a sample reveals the surface chemical composition of a material within 10 nm of thickness. In the IR spectrum of the ground sand sample (Supporting Information, Fig. s-1), major vibration bands were observed at 711.5 cm^{-1}, 854.2 cm^{-1}, 1082.2 cm^{-1}, and 1449.6 cm^{-1}. Bands at 1449.2 cm^{-1}, 854.2 cm^{-1}, 711.5 cm^{-1} can be assigned to asymmetric stretching, in-plane and out-of-plane bending modes of CO_3^{2-} [31], respectively, confirming that the major chemical component of Cancun sand is a carbonate mineral. Figure 1 is the XPS spectrum of the sand sample. In the spectrum, XPS peaks for C 1s, Ca $2p_{3/2}$, and O 1s were observed at 289.3 eV, 247.3 eV and 531.5 eV, respectively. These peaks can be assigned to C, Ca, O from $CaCO_3$ [32]. In addition, three minor peaks were observed at 132.8 eV, 102.1 eV and 43.3 eV. The peak at 132.8 eV is assigned to Sr in $SrCO_3$ and the peak at 102.1 eV is assigned to Si 2p in $CaSiO_3$ [33]. As for the peak at 43.3 eV, it could be attributed to As $3d_{5/2}$ for asenic oxide. The peak area and atomic concentration of each element are listed in Table 1. The atomic percentages of Ca and C in the sand sample were 15% and 13%, respectively. This ratio fits well to the atomic ratio of Ca and C in $CaCO_3$ (1:1). In addition to Ca and C, 2.7% of Si also exists. The chemical shift of Si 2p corresponds to SiO_3^{2-}, suggesting the presence of $CaSiO_3$ in the sand particles. In addition, trace amounts of $SrCO_3$ and some arsenic oxide were also found from Cancun sand.

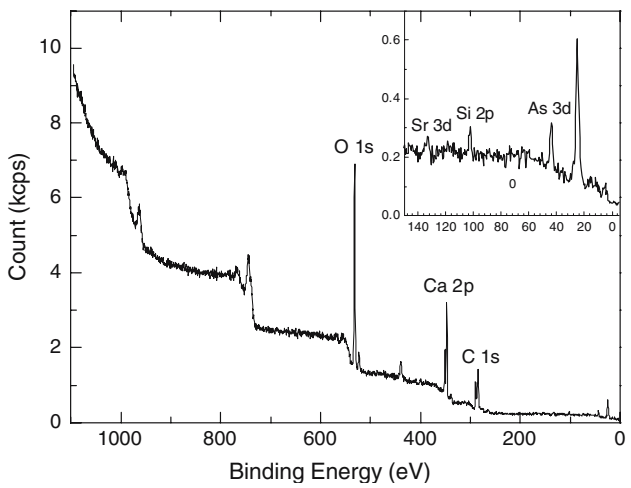

Fig. 1 XPS spectrum of Cancun sand particles

Table 2 Specific surface area, pore diameter and average pore size of Cancun sand and Florida sand

Sample	Specific surface area (m^2/g)	Pore volume (cm^3/g)	Average pore size (nm)
Cancun sand	2.259	0.004	3.4
Florida sand	0.636	0.001	3.6

Surface area and pore diameter

Figure 2 shows the sorption isotherms of N_2 that were obtained from Cancun sand and Florida sand. The specific surface area, pore volumes and average pore diameters are listed in Table 2. For both samples, hysteresis loops associated with the occurrence of pore condensation were observed. According to IUPAC classification, the hysteresis loops are characteristic features for type IV isotherms that are typically observed on mesoporous materials [34]. From the sorption isotherms, it is clear that Cancun sand is a mesoporous material. This is additionally confirmed by the fact that the average pore size of Cancun sand obtained by BJH method is 3.4 nm.

From the analysis of multi-point BET data, the specific surface area of Cancun sand was determined to be 2.259 m^2/g. This value is about 3.5 times larger than the specific surface area of Florida sand, which is 0.636 m^2/g. This value is also significantly larger than the specific surface area of Ottawa sand, which is only 0.0485 m^2/g [35], the specific surface area of natural calcite, which is 0.056 m^2/g [36], and higher than that of natural aragonite, which is 1.7 m^2/g [37]. In addition, the BET measurement showed that the pore volume of Cancun sand was 0.004 cm^3/g. As a comparison, the pore volume of Florida sand is 0.001 cm^3/g, only one quarter of Cancun sand.

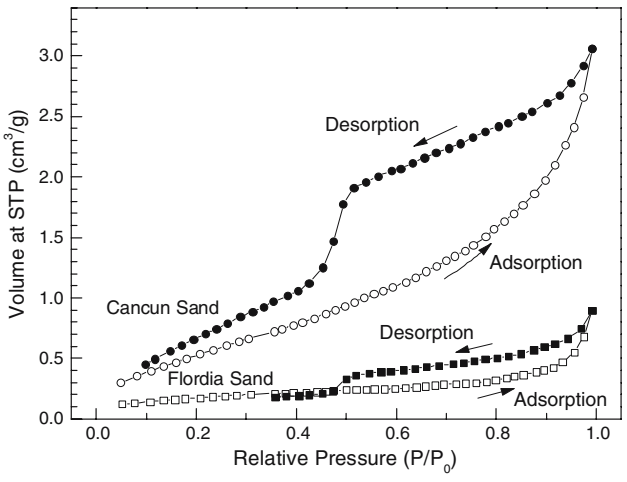

Fig. 2 Adsorption and desorption isotherms of N_2 on Cancun and Florida sand particles

At a closer look at the isotherm of Cancun sand, a delay of condensation appears in adsorption curve and a steep decrease in volume can be observed between relative pressure of 0.51 and 0.43 in desorption curve. This hysteresis phenomenon reflects the existence of ink bottle-like pores with narrow neck. For ink bottle-like pores, the wide body is filled at the vapor pressure before condensation occurs in narrow neck, which results in a delayed condensation during adsorption. On the other hand, the pores remain filled until the narrow neck is emptied first at lower vapor pressure during desorption. This empty pressure is below a characteristic percolation threshold associated with an open surface. Therefore, the desorption curve of the sorption isotherm is significantly steeper than the adsorption curve [38].

Surface morphology

The SEM images obtained from as collected sand sample were shown in Fig. 3. The images reveal that the sand surfaces have different roughness. Some surface areas of sand particles were broken by bioerosion or wave action. The apparent porous structure was exposed. From the SEM images taken on ground sand samples (Fig. 4), it was clearly shown that Cancun sand contains a large number of porous channels with the channel dimensions ranging from several nanometers to about 100 nm. Although we cannot estimate the average internal pore size of the channels from SEM analysis, the images corroborate with the results revealed by BET analysis.

Structural determination

It is well known that calcium carbonate has three anhydrous polymorphs: calcite, aragonite and vaterite [39]. These materials have the exactly same chemistry but different crystalline structures. Vaterite is very soluble in water and is rarely seen in nature. Calcite is considered to be the most stable form and is widely distributed on the earth. Calcite has a Trigonal—Hexagonal Scalenohedral crystal system. As for aragonite, it has an Orthorhombic—Dipyramidal structure and is generally thought to be unstable under normal surface pressure and temperature. However, due to biomineralization, aragonite is found frequently in environment [40].

Since Cancun sand is not soluble in water, vaterite can be ruled out from its crystalline structure. In order to identify the structure of Cancun sand, powder XRD analysis was conducted on the ground Cancun sand sample (X-ray diffraction spectrum is shown in Supporting Information, Fig. s-2). There is a series of sharp peaks observed in the spectrum, indicating the presence of crystalline structure in the sand particles. The exact peak locations are extracted and shown in Fig. s-2b. These peaks perfectly match to the ones for aragonite calcium carbonate in the Powder Diffraction File, No. 075-2230, from ICSD (see Fig. s-2c). Besides those peaks for aragonite, there is a mediate peak at 2θ of about 29° as marked in Fig. s-2a. According to ref. [31], it may be the peak arising from calcite. The aragonite structure of Cancun sand is also supported by re-examining its IR vibration bands from 600 cm^{-1} to 1,200 cm^{-1} (Supporting Information, Fig. s-1b). Typically, aragonite has a characteristic band at around 1082 cm^{-1} while calcite lacks this band. Moreover, aragonite has a doublet band at around 710 cm^{-1}, but calcite does not [31]. Both features of aragonite calcium carbonate were found in the IR spectrum of Cancun sand: one mediate band at 1082.2 cm^{-1} and one doublet band at 711.5 and 699.5 cm^{-1}. Therefore, the Cancun sand can be determined as aragonite calcium carbonate.

Other than the crystalline structure information, a broad band was found to span from 15° to 25° in the XRD spectrum of the sand sample. The baseline was also raised. Since the very fine powder was screened out before test, it is reasonable that these two observations might be caused by amorphous structure or very fine grains that exist in the sand particles.

The internal morphological structure of the Cancun sand particles was further characterized by TEM. A very thin cross section was cut from bulky material by FIB for TEM

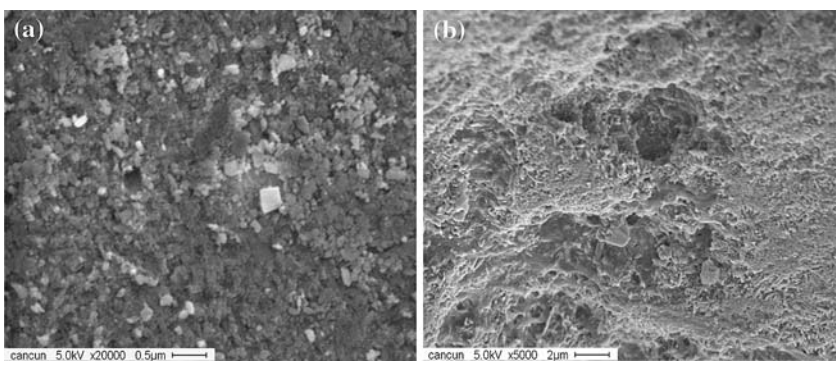

Fig. 3 SEM images of as collected Cancun sand particles with two different surface morphologies

analysis. In Fig. 5a, the uniform black area on the left side of the image is the platinum coating used to protect the surface of the sand particle. In the thin cross section area, many channels with diameter around 100 nm across the solid matrix (bright area) can be found. The magnified image (Fig. 5b) shows a strong contrast of dark and bright areas that are possibly due to the different compositions or different grain structures of sand particles. Energy dispersive X-ray spectroscopy (EDXS) analysis was used to analyze the composition of both the dark and bright areas. The results were summarized in the Supporting Information (Table s-1 and s-2). From these two tables, it can be seen that the bright area contains more than 80% of C while the atomic content of Ca is only around 10%. In contrast, there is more than 30% of Ca and around 50% of C in the dark area. Since Ca is heavier than C, more Ca will result in a darker area in TEM bright field image, which is in good agreement with TEM image shown in Fig. 5. These results suggest a heterogeneous structure of Cancun sand particles.

The grain structures of the dark and bright areas were further analyzed by electron diffraction with TEM. The diffraction patterns in Fig. 6a and b were obtained from the dark and bright areas shown in Fig. 5b, respectively. The diffraction pattern from the dark area is a twinned hexagonal like pattern. Since three aragonite crystals can group together to form a three-membered cyclic twin crystal, giving a pseudohexagonal facet [41], the pattern we observed is very likely resulted from the diffraction on this plane. On the other hand, the diffraction pattern from the bright area shows two rings and many scattered diffraction spots. Since the rings in diffraction pattern result from the existence of very fine grains, this diffraction pattern suggests that the bright area contains fine crystalline with different orientations. This conclusion was further supported by high resolution TEM image of sand particles (Supporting Information, Figure s-4): different orientations of the grains at nanometer size range were observed. Therefore, both composition and structure differences contribute to the dark–bright contrast in TEM image. This verified that the sand has a chemically and structurally heterogeneous structure.

Nanoparticle adsorption

Gold nanoparticles are one of the most extensively studied nanoparticle materials [42]. Gold nanoparticles with diameters around a few nanometers can be conveniently

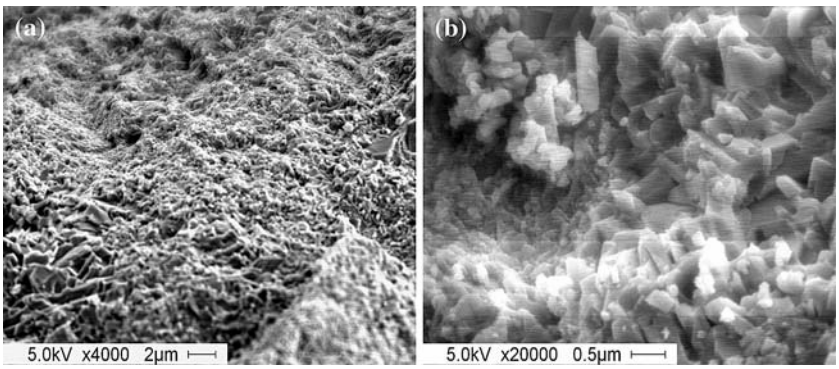

Fig. 4 SEM images of ground Cancun sand particles: (**a**) at low magnification; (**b**) at high magnification

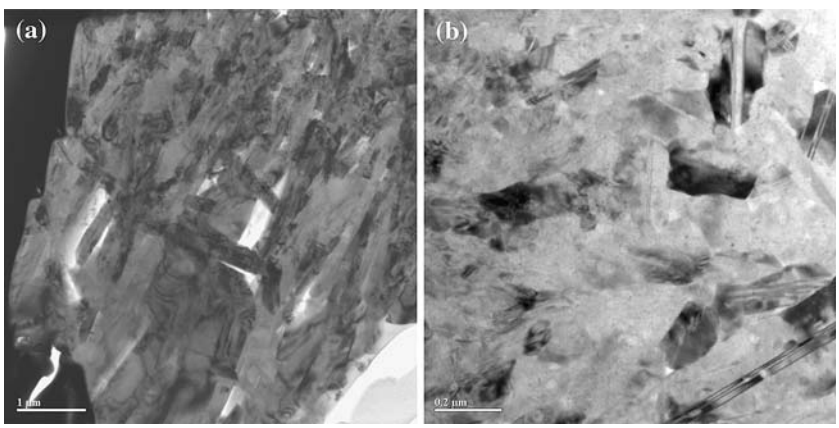

Fig. 5 TEM image of the cross section of Cancun sand particles: (**a**) at low magnification; (**b**) at high magnification

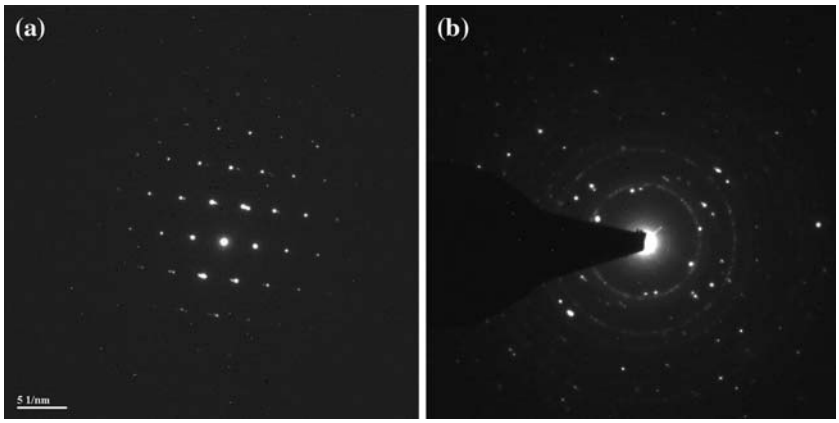

Fig. 6 X-ray diffraction pattern obtained from a cross-section of a Cancun sand particle

prepared by wet chemical methods such as Brust-Schiffrin reaction [43, 44]. Because of their extremely small dimensions, we believe that it can be used as a probe to explore the internal structure of the sand particles. Since gold is a heavy metal and gold nanoparticles can be easily imaged by TEM, the TEM image of sand particle after immobilization of gold nanoparticles could help us to examine the diffusion of gold nanoparticle in porous channels of the sand and reveals the structure, dimension and distribution of internal channels inside the sand particles.

After dispersing ground sand into the gold nanoparticle solution, it was found that the gold nanoparticles were absorbed into the sand within a few seconds. The gold nanoparticles solution changed from strong black to very light brown and transparent. Meanwhile, the sand particles changed color from creamy white to dark gray because of the deposition of gold nanoparticles. It is further noticed that the adsorbed gold nanoparticles were trapped very well in the sand as the particles could not be washed off even by a copious amount of solvents. In a comparison experiment with Florida sand, gold nanoparticles were not adsorbed by the sand. This interesting property of Cancun sand suggests their potential application in controlling pollution that may be caused by nanoparticles or other related hazardous chemical materials.

In order to study the distribution of the gold nanoparticles in sand, a thin layer of cross section of the sand was prepared by FIB technique and examined by TEM. Figure 7a shows the outer surface area of the sand particles, protected by a platinum coating (dark edge in the image) and Fig. 7b and c are the images obtained from inner area of sand particle. The black dots appeared in these pictures showed the presence of gold nanoparticles. Gold nanoparticles are observed both on the surface (Fig. 7a) and inside the sand particles (Fig. 7b and c). This confirms that nanoparticles not only adsorb onto the surface of the sand, but also diffuse into the porous channels of the sand particles. Interestingly, in some cases, gold nanoparticles formed some highly ordered linear alignments in some areas, suggesting that nano-size channels with diameter approximately 5 nm exist inside sand particles. This result is in good agreement with results from the BET measurement.

The gold nanoparticles used here have an organic thiol ligand layer on the particle surface, which is used to prevent the aggregation of the gold nanoparticles and also to make the nanoparticles soluble in organic solvent such as dichloromethane. The surface of these gold nanoparticles has a low surface energy. The strong adsorption tendency of gold nanoparticles to sand particles indicates that the surface of the sand particles has good affinity towards low surface energy materials. The results of this study suggest that Cancun sand particles may be used as an excellent filtration material to remove both hydrophobic and hydrophilic nano- and microscopic particles for a wide range of purification purposes.

Sand particle–polymer interface property

Because of the porous structure and low surface energy of the Cancun sand particles, we surmised that these sand particles could form a good adhesion interface with polymers such as PMMA, as suggested in the Introduction. In order to prove this hypothesis, polymer composite films that contained Cancun sand or Florida sand were prepared and the so-formed sand particle–polymer interface was examined by SEM. From the SEM micrographs as shown in Fig. 8, clear differences between the interfaces of two different composite materials can be observed. For Florida sand–PMMA composite, there is almost no bonding between the sand particles and polymer matrix. In contrast, there is a strong adhesion between Cancun sand particles and PMMA layer. At the interface, the sand particle and the polymer seemed to be ‘‘fused’’ together. We believe that it is due to the penetration of hydrophobic polymer molecules

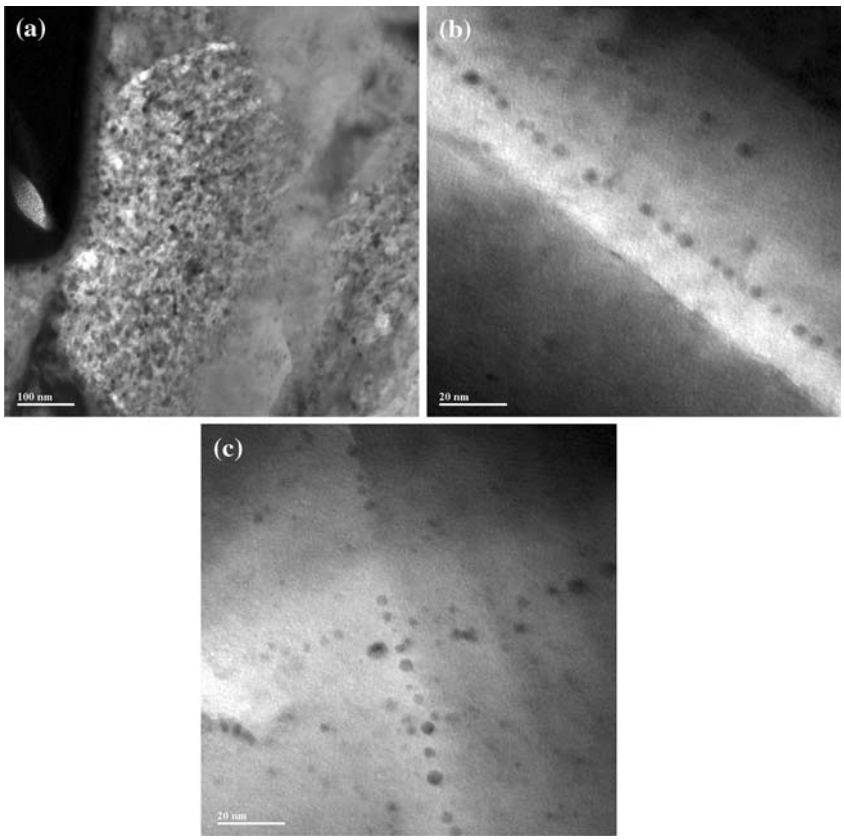

Fig. 7 TEM images of the cross-sections of Cancun sand particles after adsorption of gold nanoparticles

into the similarly hydrophobic porous sand particles. A good interface adhesion between filler particles and polymer matrix is vital for a good mechanical property of a composite material. The results described here suggest a promising potential application of Cancun sand for polymer composite material development (Fig. 8)

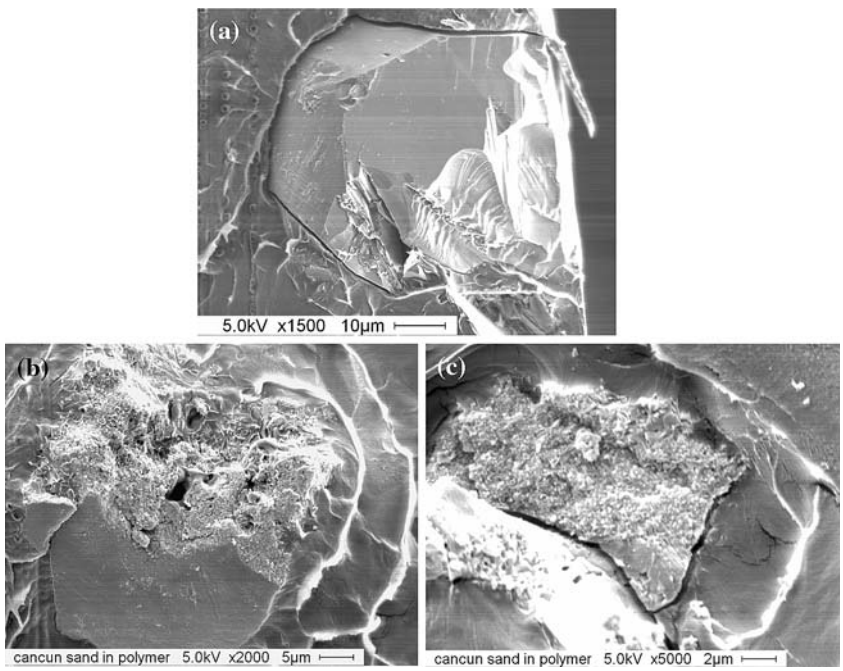

Fig. 8 SEM images of interfaces of (**a**) Florida sand particle–PMMA composite, and (**b**) and (**c**) Cancun sand particle–PMMA composite

Conclusion

The composition, surface morphology and internal structure of Cancun sand particles were characterized by various advanced spectroscopic and microscopic techniques. The XPS and IR results showed that Cancun sand is mainly composed of calcium carbonate, which is widely observed in tropical and subtropical environments. The XRD analysis revealed that Cancun sand is aragonite, which has an Orthorhombic—Dipyramidal crystal structure. The large specific surface area and pore volume determined by BET measurement indicated that Cancun sand is a porous material with an average pore size of 3.4 nm and a specific surface area of 2.259 m^2/g. SEM and TEM confirmed the porous structure of Cancun sand and in addition revealed that there exist channels with size ranging from several to less than 100 nm inside the sand particles.

Cancun sand showed strong ability in absorbing gold nanoparticles that are covered with hydrophobic ligands, indicating that the sand particles have strong affinity towards hydrophobic particles and other chemical species. This property was also confirmed by a good adhesion at the interface of sand–PMMA composite. All these properties suggest that Cancun sand as a natural porous material may find a wide range of potential applications, particularly in the areas of filtration, catalysis, pollution control and new composite material development.

Acknowledgements We want to thank Dr. Joseph Brennan for collecting the sand samples for this project. Partial work reported here was supported by National Science Foundation CAREER award (DMR 0552295) and National Science Foundation NIRT award (DMI 0506531).

References

1. Davis ME (2002) Nature 417:813
2. Zhao XS, Bao XY, Guo W, Lee FY (2006) Mater Today 9:32
3. Vago R, Plotquin D, Bunin A, Sinelnikov I, Atar D, Itzhak D (2002) J Biochem Biophys Methods 50:253
4. Torgersen AN, Jorgensen SW (2006) US Patent 2006097221
5. Sapelkin AV, Bayliss SC, Unal B, Charalambou A (2006) Biomaterials 27:842
6. Saupe GB, Zhao Y, Bang J, Yesu NR, Carballo GA, Ordonez R, Bubphamala T (2005) Microchem J 81:156
7. Gottlieb L (2005) Reactive Func Poly 63:107
8. Teng X, Liang X, Rahman S, Yang H (2005) Adv Mater 17:2237
9. Palmqvist AEC, Iversen BB, Zanghellini E, Behm M, Stucky GD (2004) Angew Chem Int Ed 43:700
10. Corma A, Diaz-Cabanas MJ, Martinez-Triguero J (2002) Nature 418:514
11. Corma A, Nemeth L, Renz M, Valencia S (2001) Nature 412:423
12. Stein A (2003) Adv Mater 15:763
13. Dybtsev DN, Chun H, Yoon SH, Kim D, Kim K (2003) J Am Chem Soc 126:32
14. Millward AR, Yaghi OM (2005) J Am Chem Soc 127:17998
15. Manning DAC (1995) Introduction to industrial minerals. Chapman & Hall, London
16. Zhao Y, Cao D, Liu L, Jin W (2006) Water Environ Res 78:392
17. Christensen AN, Lundtoft B, Madsen IC (2001) J Am Chem Soc 84:878
18. Ai-Ghouti MA, Khraisheh MAM, Allen SJ, Ahmad MN (2003) J Environ Manage 69:229
19. Nyer K (1992) Ground water treatment technology, 2nd edn. Van Nostrand Reinhold
20. Rahmana MA, Ahsana S, Kanecoa S, Katsumataa H, Suzukib T, Ohtaa K (2005) J Environ Manage 74:107
21. Katti KS (2004) Colloids Surf B 39:133
22. Ratner MA, Ratner D, Ratner M (2003) Nanotechnology: a gentle introduction to the next big idea. Prentice Hall PTR, New Jersey
23. Tucker ME, Wright UP (1990) Carbonate sedimentology. Blackwell Science Ltd., p 100
24. Moulder JF, Stickle WF, Sobol PE, Bomben KD (1995) Handbook of X-ray photoelectron spectroscopy. Perkin-Elmer Corporation
25. Williams DB, Carter CB (1996) Transmission electron microscopy, vol 4. Plenum Press, New York, p 600
26. Giannuzzi LA, Drown JL, Brown SR, Irwin RB, Stevie FA (1997) Mater Res Soc Symp Proc 480:19
27. Giannuzzi LA, Drown JL, Brown SR, Irwin RB, Stevie FA (1998) Micros Res Tech 41:285
28. Brunauer S, Emmett PH, Teller E (1938) J Am Chem Soc 60:309
29. Barrett EP, Joyner LG, Halenda PP (1951) J Am Chem Soc 73:373
30. Worden JG, Dai Q, Shaffer A, Huo Q (2004) Chem Mater 16:3748
31. Chakrabarty D, Mahapatra SJ (1999) Mater Chem 9:2953
32. Christie AB, Lee J, Sutherland I, Walls JM (1983) Appl Surf Sci 15:224
33. Wagner CD, Passoja DE, Hillery HF, Kinisky TG, Six HA, Jansen WT, Taylor JA (1982) J Vac Sci Tech 21:933
34. Sing KSW, Everett DHW, Hall HRA, Moscou L, Pierotti RA, Rouquerol J, Siemieniewska T (1985) Pure Appl Chem 57:603
35. Slater L, Ntarlagiannis D, Wishart D (2006) Geophysics 71:A1
36. Zwingmann N, Mito S, Sorai M, Ohsumi T (2005) Oil Gas Sci Tech Rev IFP 60:249
37. Wypych G (2000) Handbook of fillers—a definitive user's guide and databook, 2nd edn. ChemTec Publishing, p 255
38. Thommers M, Smarsly B, Groenewolt M, Ravikovitch PI, Neimark AV (2006) Langmuir 22:756
39. Coelfen HCO (2003) Colloid Interf Sci 8:23
40. Rohleder J, Kroker E, Tegethoff FW (2001) Calcium carbonate: from the cretaceous period into the 21st century. Birkhauser Verlag, Seitzerland, p 14
41. Shindo H, Kwak M (2005) Phys Chem Chem Phys 7:691
42. Daniel M-C, Astruc D (2004) Chem Rev 104:293
43. Brust M, Walker M, Bethell D, Schiffrin DJ, Whyman R (1994) J Chem Soc Chem Comm:801
44. Hostetler MJ, Wingate JE, Zhong C-J, Harris JE, Vachet RW, Clark MR, Londono JD, Green SJ, Stokes JJ, Wignall GD, Glish GL, Porter MD, Evans ND, Murray RW (1998) Langmuir 14:7